



Polymorphism and phase transformation in the dimethyl sulfoxide solvate of 2,3,5,6-tetrafluoro-1,4-diiodobenzene

Andrew D. Bond* and Chris L. Truscott

Department of Chemistry, University of Cambridge, Lensfield Road, Cambridge CB2 1EW, England. *Correspondence e-mail: adb29@cam.ac.uk

Received 13 April 2020

Accepted 24 April 2020

Edited by A. L. Spek, Utrecht University, The Netherlands

Keywords: halogen bonding; polymorphism; variable temperature; crystal structure; phase transformation; *PIXEL*.**CCDC references:** 1998986; 1998985; 1998984**Supporting information:** this article has supporting information at journals.iucr.org/c

A new polymorph (form II) is reported for the 1:1 dimethyl sulfoxide solvate of 2,3,5,6-tetrafluoro-1,4-diiodobenzene (TFDIB-DMSO or $C_6F_4I_2 \cdot C_2H_6SO$). The structure is similar to that of a previously reported polymorph (form I) [Britton (2003). *Acta Cryst.* **E59**, o1332–o1333], containing layers of TFDIB molecules with DMSO molecules between, accepting $I \cdots O$ halogen bonds from two TFDIB molecules. Re-examination of form I over the temperature range 300–120 K shows that it undergoes a phase transformation around 220 K, where the DMSO molecules undergo re-orientation and become ordered. The unit cell expands by *ca* 0.5 Å along the *c* axis and contracts by *ca* 1.0 Å along the *a* axis, and the space-group symmetry is reduced from *Pnma* to *P2₁2₁2₁*. Refinement of form I against data collected at 220 K captures the (average) structure of the crystal prior to the phase transformation, with the DMSO molecules showing four distinct disorder components, corresponding to an overlay of the 297 and 120 K structures. Assessment of the intermolecular interaction energies using the *PIXEL* method indicates that the various orientations of the DMSO molecules have very similar total interaction energies with the molecules of the TFDIB framework. The phase transformation is driven by interactions between DMSO molecules, whereby re-orientation at lower temperature yields significantly closer and more stabilizing interactions between neighbouring DMSO molecules, which lock in an ordered arrangement along the shortened *a* axis.

1. Introduction

The molecule 2,3,5,6-tetrafluoro-1,4-diiodobenzene (TFDIB) is a common halogen-bond donor (Metrangolo & Resnati, 2001; Cavallo *et al.*, 2016). The work described in this article originated from a cocrystal screening, where TFDIB was combined with a series of potential halogen-bond acceptors in dimethyl sulfoxide (DMSO) solution. Crystals of TFDIB-DMSO (see Scheme) were quite commonly obtained from these experiments, some of which were found to be different from a previously reported crystal structure at 297 K [Britton, 2003; Cambridge Structural Database (CSD; Groom *et al.*, 2016) refcode IKIFOX]. We refer to the previously reported structure (IKIFOX) as form I and the newly obtained polymorph as form II. The structures are similar and we suspected at first that form II might have arisen from a phase transformation on cooling of form I in the N_2 cryostream during single-crystal data collection. We therefore obtained crystals of form I and measured them at various temperatures. We did not find any transformation of form I to form II, but instead observed re-orientation of the DMSO molecules in form I to give a further new structure measured at 120 K. We describe herein the various crystal structures of TFDIB-DMSO and the

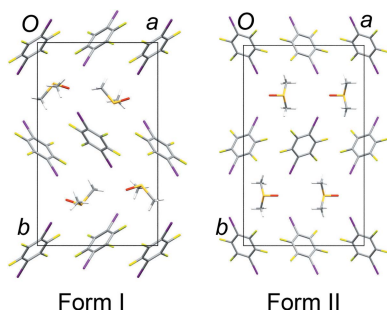


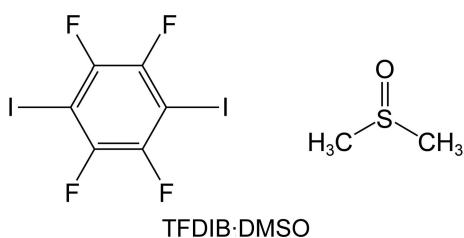
Table 1
Experimental details.

For all structures: $C_6F_4I_2 \cdot C_2H_6OS$, $M_r = 479.99$, $Z = 4$. Experiments were carried out with Mo $K\alpha$ radiation using a Nonius KappaCCD diffractometer. Absorption was corrected for by multi-scan methods (SORTAV; Blessing, 1995). H-atom parameters were constrained.

	Form II	Form I (120 K)	Form I (220 K)
Crystal data			
Crystal system, space group	Orthorhombic, $Pnma$	Orthorhombic, $P2_12_12_1$	Orthorhombic, $Pnma$
Temperature (K)	180	120	220
a, b, c (Å)	12.8308 (6), 21.3307 (12), 4.6463 (2)	10.6731 (2), 18.0023 (5), 6.5470 (2)	11.6799 (4), 18.2664 (8), 6.0984 (2)
V (Å ³)	1271.65 (11)	1257.94 (5)	1301.09 (8)
μ (mm ⁻¹)	5.14	5.19	5.02
Crystal size (mm)	0.14 × 0.14 × 0.14	0.12 × 0.10 × 0.10	0.12 × 0.10 × 0.10
Data collection			
T_{min}, T_{max}	0.411, 0.464	0.475, 0.599	0.541, 0.611
No. of measured, independent and observed [$I > 2\sigma(I)$] reflections	7999, 1463, 952	11512, 2834, 2141	8062, 1520, 948
R_{int}	0.049	0.089	0.057
$(\sin \theta/\lambda)_{max}$ (Å ⁻¹)	0.649	0.649	0.650
Refinement			
$R[F^2 > 2\sigma(F^2)], wR(F^2), S$	0.033, 0.086, 1.01	0.043, 0.078, 0.99	0.038, 0.082, 1.06
No. of reflections	1463	2834	1520
No. of parameters	83	148	112
No. of restraints	0	0	71
$\Delta\rho_{max}, \Delta\rho_{min}$ (e Å ⁻³)	1.01, -1.27	0.91, -1.18	0.62, -0.69
Absolute structure	–	Refined as an inversion twin.	–
Absolute structure parameter	–	0.19 (5)	–

Computer programs: COLLECT (Nonius, 1998), HKL SCALEPACK (Otwinowski & Minor, 1997), HKL DENZO (Otwinowski & Minor, 1997), SHELXT (Sheldrick, 2015a), SHELXL2018 (Sheldrick, 2015b) and Mercury (Macrae *et al.*, 2020).

application of dispersion-corrected DFT and PIXEL calculations (Gavezzotti, 2002, 2003, 2011) to examine the DMSO re-orientation on cooling of form I.



2. Experimental

2.1. Synthesis and crystallization

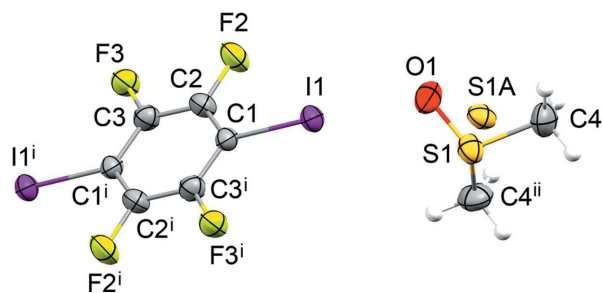
Crystals of forms I and II were produced during a sequence of attempted cocrystallization experiments. TFDIB and an anticipated coformer were dissolved in DMSO, and crystals were produced by vapour diffusion of water into the solution under ambient conditions. Form I (CSD refcode IKIFOX; Britton, 2003) was obtained frequently, while crystals of form II were obtained specifically from a 2:3 mixture of TFDIB and melamine ($C_3H_6N_6$). The structure of form II was measured at 180 K, whereby the crystals were plunged directly from ambient conditions into a cold N_2 stream. Similar treatment of form I resulted in cracking and the loss of single crystallinity. Analysis of form I was therefore made by placing the crystal initially into the N_2 stream at room temperature, followed by slow cooling as described in §3.2.

2.2. Refinement

Crystal data, data collection and structure refinement details are summarized in Table 1. Determination of the structure of form II at 180 K was straightforward. The DMSO molecule in the asymmetric unit is situated with its internal mirror plane on the crystallographic mirror plane at $x_{1/4}, z$ in the space group $Pnma$ (Fig. 1). The S atom is split into two atomic sites within the mirror plane, with refined site occupancies of 0.424 (5) and 0.576 (5).

For form I at 120 K, the space group is clearly $P2_12_12_1$, with the DMSO molecule ordered on a general equivalent position and with no significant residual electron density in the vicinity of the molecule (Fig. 2). The structure was refined as an inversion twin with the Flack parameter converging to 0.19 (5). The applied unit-cell setting and origin (placing the 2_1 screw axes at $x_{1/2}, 1/2; 0, y, 0; 1/2, 0, z$) are nonstandard for the space group $P2_12_12_1$ [Hall symbol: $P\ 2ac\ 2n$], but chosen to maintain the relationship with the form I structure at 297 K (IKIFOX) in its standard setting of $Pnma$.

For the refinement of form I after cooling to 220 K, the DMSO molecule was modelled in four orientations (Fig. 3). Two orientations are similar to those in form II, with the internal mirror plane of the DMSO molecule coincident with the mirror plane at $x_{1/4}, z$ in the space group $Pnma$, and with the S atom split into two atomic sites with refined site occupancies of 0.356 (3) and 0.191 (3). A further orientation is defined with the S atom out of the mirror plane with a refined site occupancy of 0.226 (2), giving two further orientations of the DMSO molecule. The site occupancies of the three refined

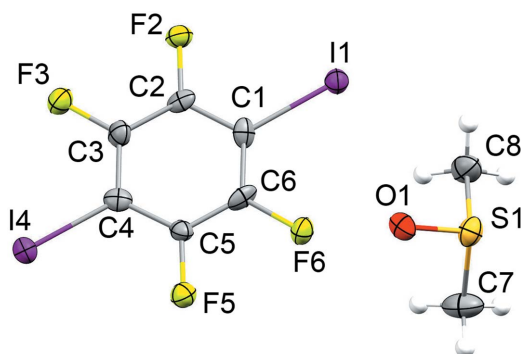

Figure 1

The molecular structure of form II at 180 K, with displacement ellipsoids at the 50% probability level for non-H atoms. The site-occupancy factors for atoms S1 and S1A are 0.424 (5) and 0.576 (5), respectively. Only the major component is shown as connected. [Symmetry codes: (i) $-x + 1, -y + 1, -z$; (ii) $x, -y + \frac{3}{2}, z$.]

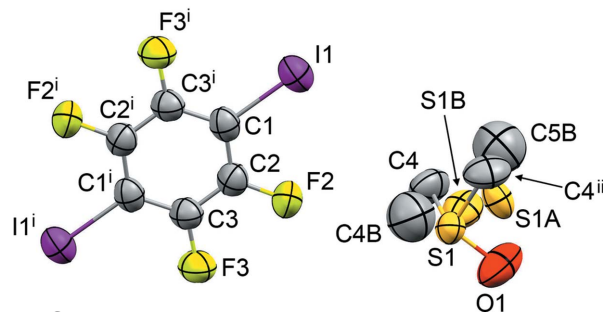
components were tightly restrained to sum to unity (using SUMP in *SHELXL*; Sheldrick, 2015b) and restraints were applied to all S–O, S–C and C··C distances. All non-H atoms were refined with anisotropic displacement parameters, restrained to resemble isotropic behaviour (ISOR in *SHELXL*). An extinction coefficient was refined. In all structures, the H atoms of the DMSO molecule were placed in idealized positions, with $U_{\text{iso}}(\text{H}) = 1.5U_{\text{eq}}(\text{C})$. The methyl groups were not permitted to rotate around their local threefold axes, since this prevented convergence of the refinement. The structure and refinement details are presented in Table 1.

2.3. Computational details

The crystal structures were energy-minimized with dispersion-corrected density functional theory (DFT-D) using the *CASTEP* module (Clark *et al.*, 2005) in *Materials Studio* (Accelrys, 2011). The PBE functional (Perdew *et al.*, 1996) was applied with a plane-wave cut-off energy of 520 eV, in combination with the Grimme semi-empirical dispersion correction (Grimme, 2006). The structures in the space group *Pnma* were reduced to the space group *P2₁2₁2₁* to allow the definition of complete molecules, so all optimizations were carried out in *P2₁2₁2₁*. The unit-cell parameters were constrained to the experimental values. For the disordered structures, models were built containing the various individual


Figure 2

The molecular structure of form I at 120 K, with displacement ellipsoids at the 50% probability level for non-H atoms.


Figure 3

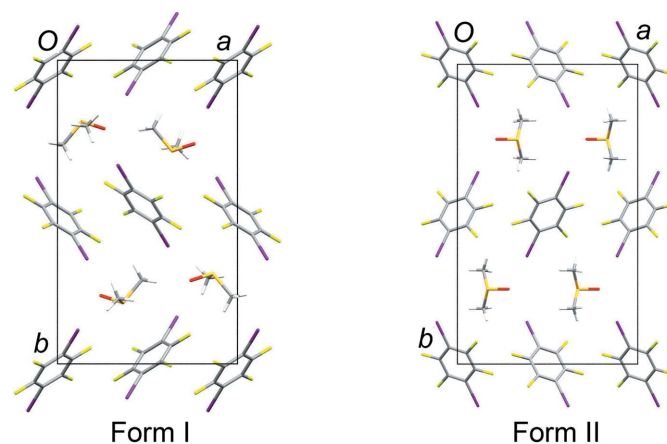
The molecular structure of form I at 220 K, with displacement ellipsoids at the 50% probability level. H atoms have been omitted from the disordered DMSO molecule for clarity, and only the major component is shown as connected. The site-occupancy factors for the DMSO components containing atom S1, S1A and S1B are 0.356 (3), 0.191 (3) and 0.226 (2), respectively. [Symmetry codes: (i) $-x + 1, -y + 1, -z - 1$; (ii) $x, -y + \frac{3}{2}, z$.]

DMSO components and optimized separately. The DFT-D-optimized structures were used as input for the *PIXEL* module of the CSP package (Gavezzotti, 2002, 2003, 2011) to examine the energies of the pairwise intermolecular interactions. The calculated interaction energies are estimated to have accuracy within the range *ca* ± 3 kJ mol⁻¹.

3. Results and discussion

3.1. Structure of form II

Both form I and form II adopt structures with a layered arrangement of TFDIB molecules in the (020) planes (Fig. 4). The DMSO molecules occupy sites between these layers. The difference between forms I and II reveals some flexibility in the structure of the TFDIB layers within the crystalline state. Taking one layer and looking side-on to the molecules [projecting onto the (110) planes], form II shows an approximately perpendicular arrangement of molecules, while form I shows a smaller angle between the molecular planes (Fig. 5).


Figure 4

The form I and II structures, viewed along the *c* axis, showing layers of TFDIB molecules in the (020) planes. The arrangement of TFDIB molecules in form I is closely comparable at 297 and 120 K (the 120 K structure is shown).

This difference is reflected in the unit-cell parameters (Table 1), particularly in the substantially shorter c axis for form II. The sites occupied by the DMSO molecules between the TFDIB layers in form II are substantially similar to those in form I, as described in §3.2. The DMSO molecules lie on the crystallographic mirror planes at $x_{\frac{1}{4}}, z$ and $x_{\frac{3}{4}}, z$, accepting $I \cdots O$ halogen bonds from two TFDIB molecules either side of the mirror plane [$I1 \cdots O1 = 2.847(2) \text{ \AA}$]. Disorder is present in the manner described for form I at 297 K (§3.2), with the DMSO molecules adopting orientations **A** and **B** with refined site occupancies of 0.576 (5) and 0.424 (5), respectively.

3.2. Temperature-dependent structure of form I

The previously-reported structure of form I at 297 K (Britton, 2003; CSD refcode IKIFOX) exhibits two orientations of the DMSO molecules (labelled **A** and **B**), as illustrated in Fig. 6. We obtained an identical disorder model in our own refinements at 300 K (not reported). Each DMSO molecule lies on a mirror plane in a pocket between eight TFDIB molecules. The position of the O atom is approximately consistent in both orientations, acting as an acceptor for $I \cdots O$ halogen bonds from two TFDIB molecules ($I \cdots O \simeq 2.80\text{--}2.90 \text{ \AA}$). In orientation **A**, the $S\text{--}CH_3$ bond vectors point approximately perpendicular to the planes of two TFDIB molecules. In orientation **B**, the $S\text{--}CH_3$ bonds lie closer to parallel to the TFDIB planes (Fig. 6). Thus, the DMSO molecules are ‘anchored’ by the $I \cdots O$ halogen bonds, but the $S\text{--}CH_3$ bond vectors can point either perpendicular or parallel to the neighbouring TFDIB rings. In the structure reported by Britton (2003), the refined site occupancies for **A** and **B** were 0.620 (17) and 0.380 (17), respectively.

On cooling of form I to 220 K, the unit cell and positions of the TFDIB molecules remain comparable to those at 297 K and both DMSO orientations **A** and **B** remain present. However, new peaks arise in the electron density corresponding to further orientations of the DMSO molecules. At first it was difficult to unravel this disorder, but the situation

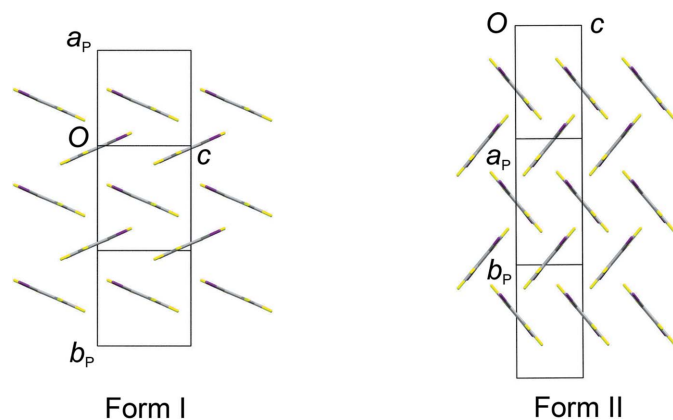


Figure 5
A single layer of TFDIB molecules, looking side-on to the molecules [projecting approximately onto the (110) planes]. Form I shows a smaller angle between the molecular planes and has a longer c axis. The arrangement of TFDIB molecules in form I is closely comparable at both 297 and 120 K (the 120 K structure is shown).

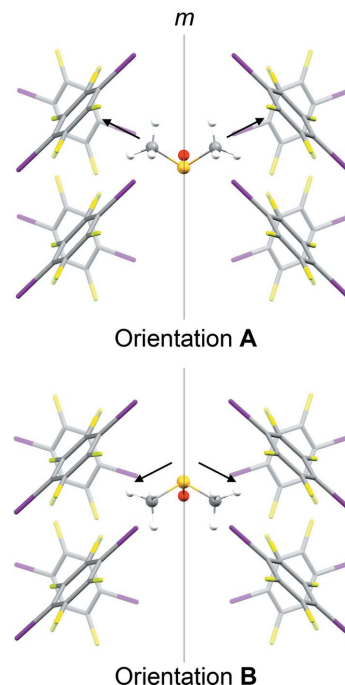


Figure 6
Two orientations (**A** and **B**) of the DMSO molecule in the form I structure at 297 K (Britton, 2003). The molecules occupy a site between eight TFDIB molecules. The arrows indicate the directions of the $S\text{--}CH_3$ bond vectors, *i.e.* perpendicular (**A**) or parallel (**B**) to the planes of the two TFDIB molecules at the top in the front plane.

became clear after the structure was determined at 120 K. The disorder at 220 K corresponds to *four* DMSO orientations, comprising **A**, **B** and two new (symmetry-related) orientations described below for the 120 K structure. A significant feature of the form I structure at 220 K is that its unit-cell parameters and TFDIB positions remain comparable to those at 297 K (Britton, 2003). Thus, cooling of the structure from 297 to 220 K causes some re-orientation of the DMSO molecules, but

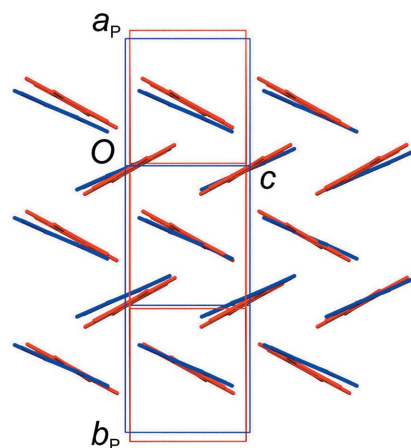


Figure 7
Overlay of a single layer of TFDIB molecules [projecting approximately onto the (110) planes] in the form I structure at 297 K (red; Britton, 2003) and 120 K (blue). The change in the unit-cell parameters is clear, but the positions of the TFDIB molecules change only very slightly.

Table 2

Total intermolecular interaction energies (kJ mol^{-1}) involving the DMSO molecules in form I, calculated using the *PIXEL* method, applied to the DFT-D-optimized structures.

Structure	Disorder component	Refinement temperature (K)	<i>a</i> (Å)	<i>b</i> (Å)	<i>c</i> (Å)	E_{tot} DMSO–TFDIB	E_{tot} DMSO–DMSO
Form I	A	297	11.819	18.418	6.075	−107.4	−25.0
Form I	B	297	11.819	18.418	6.075	−112.0	−27.4
Form I	C	120	10.673	18.002	6.547	−109.8	−44.6

the crystal does not yet appear to have undergone any phase transformation.

After cooling the crystal slowly (*ca* 1 K min^{-1}) to 120 K, the structure changes clearly from the 297 and 220 K structures. The unit cell expands by *ca* 0.5 Å along the *c* axis and contracts by *ca* 1.0 Å along the *a* axis. Looking side-on to the TFDIB molecules in one layer shows only a very subtle change compared to the 297 K structure (Fig. 7). However, the DMSO molecules are ordered and the space-group symmetry is reduced to $P2_12_12_1$. The DMSO orientation (labelled **C**, Fig. 8) retains essentially the same O-atom position, anchored by the $\text{I} \cdots \text{O}$ halogen bonds [$\text{I1} \cdots \text{O1}^{\text{i}} = 2.874(7) \text{ Å}$ and $\text{I4} \cdots \text{O1}^{\text{ii}} = 2.871(7) \text{ Å}$; symmetry codes: (i) $x, y, z - 1$; (ii) $-x, y - \frac{1}{2}, -z + 1$]. Compared to orientations **A** and **B** (Fig. 6), the molecule rotates approximately around its S–O bond. One of the S–CH₃ bond vectors retains a position comparable to orientation **A**, with a ‘perpendicular’ approach to the face of the neighbouring TFDIB molecule. The other adopts a new position pointing approximately along the *c* axis, between TFDIB molecules. Although the symmetry of the structure is clearly reduced to $P2_12_12_1$, the TFDIB molecules retain the effective mirror symmetry of the *Pnma* structure, so that two locally equivalent DMSO orientations can be envisaged, with the S–CH₃ bond pointing towards the face of either TFDIB molecule related by the local mirror symmetry (Fig. 8). Neighbouring DMSO molecules along the *a* axis alternate in this respect (visible in Fig. 4), and the two additional components seen in the 220 K structure correspond to an overlay of these two orientations. It appears from the partial observation of orientation **C** at 220 K that some degree of DMSO reorientation can be tolerated within the ‘high-temperature’ TFDIB framework in form I, but the DMSO re-orientation ultimately drives the phase transformation to the ordered ‘low-temperature’ structure.

Additional temperature-dependent measurements were made to examine the unit-cell parameters in the region of the phase transformation. A crystal of form I was cooled from 300 to 200 K at a rate of *ca* 2 K min^{-1} , with the unit cell determined at 10 K intervals. The unit-cell volume (Fig. 9*a*) shows an approximately linear decrease over the range 300→230 K, but a clear change of gradient occurs between 230 and 220 K, suggesting that reorientation of the DMSO molecules begins to take place significantly around this temperature. Clear discontinuities are evident for both the *a* and the *c* axes (Fig. 9*b*) between the measurements made at 220 K (resembling the 297 K structure) and 210 K (resembling the 120 K structure), suggesting that the reorientation is largely complete by 210 K. Hence, the disordered structure at 220 K

captures the (average) structure of the crystal mid-transformation.

3.3. DFT-D and *PIXEL* calculations

To investigate the energetics of the associated intermolecular interactions, models were constructed containing the various DMSO components and optimized using dispersion-corrected DFT calculations (DFT-D; see *Experimental*, §2). The purpose of the DFT-D step is to produce a model with an optimized representation of the disordered solvent molecules, where the geometry from the X-ray refinement is likely to be less well defined. The pairwise interactions in the optimized structures were analysed using the *PIXEL* approach (Gavezzotti, 2002, 2003, 2011). The principal interest is the total interaction energy between the DMSO molecules and its neighbours for orientations **A**, **B** and **C** in the form I structure. In each structure, the pairwise interactions sorted by centroid–centroid distance show a clear set of eight DMSO–TFDIB interactions, as indicated in Figs. 6 and 8, with no other DMSO–TFDIB interactions having significant interaction energy. Similarly, each structure shows a clear set of six significant DMSO–DMSO interactions, which are directly comparable between the structures. Table 2 shows the sums of the total energies for these sets of interactions. It is evident

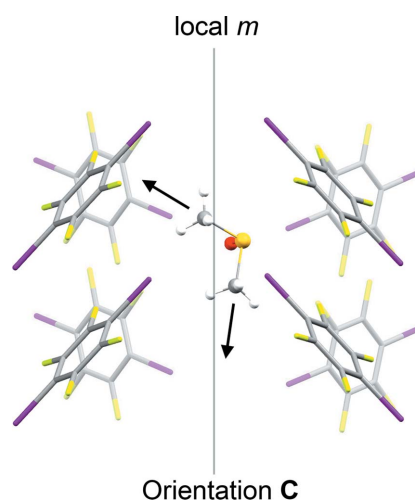


Figure 8
Orientation **C** for the DMSO molecule in the form I structure at 120 K. The arrows indicate the directions of the S–CH₃ bond vectors: one is equivalent to orientation **A** (Fig. 6), while one is distinct, pointing between TFDIP molecules. Due to the local mirror symmetry, two locally equivalent orientations are possible for the DMSO molecule, pointing either to the left or to the right in the diagram; these orientations alternate for neighbouring molecules along the *c* axis (Fig. 4).

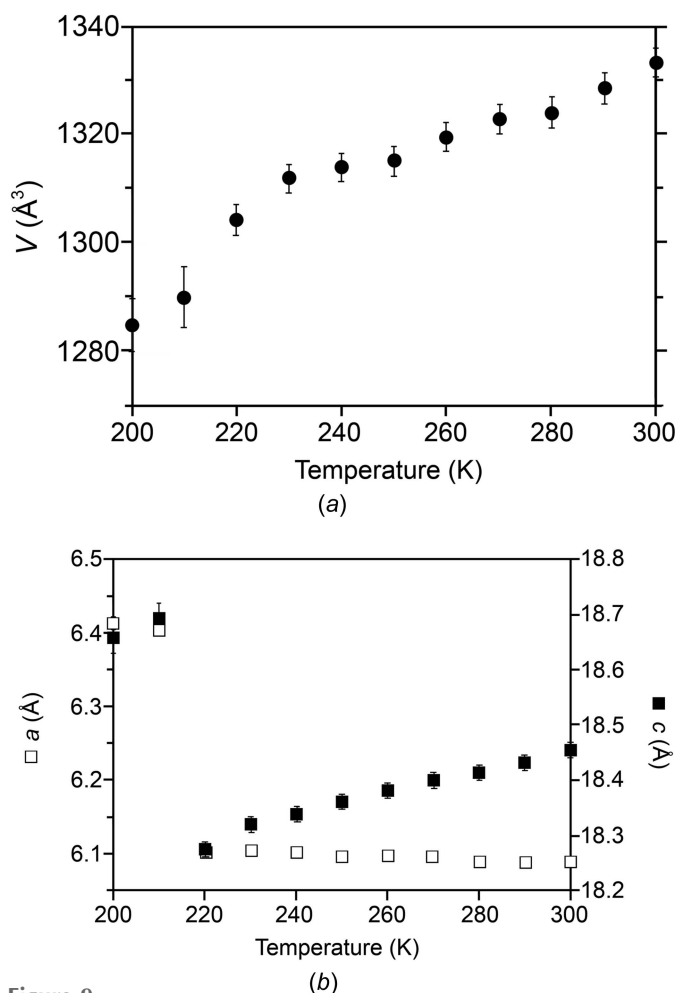


Figure 9 Variation in (a) the unit-cell volume (●) and (b) the *a* (□) and *c* (filled □) axis lengths over the temperature range 300→200 K for form I. Error bars (where visible) are drawn at $\pm(3 \times \text{s.u.})$. The clear discontinuities in the axis lengths correspond to the phase transformation from the ‘high-temperature’ TFDIB framework to the ‘low-temperature’ framework.

that the total interaction energy between DMSO and the TFDIB framework changes little between orientations **A**, **B** and **C**. Orientation **B** appears slightly favoured over orientation **A** in the form I structure at 297 K.¹ For orientation **C**, however, the calculations give a clear indication: orientation **C** is favoured on account of significantly more stabilizing interactions between the DMSO molecules. In particular, the interaction between DMSO molecules along the *a* axis (Fig. 4) has a centroid–centroid distance *ca* 0.5 Å shorter than any other DMSO–DMSO interaction and is particularly stabilizing ($E_{\text{tot}} = -17.3 \text{ kJ mol}^{-1}$). It appears that this interaction drives the ordering of the DMSO molecules, resulting in the *ca* 1.0 Å contraction of the *a* axis and symmetry reduction to the space group $P2_12_12_1$. The DMSO reorientation takes place within a TFDIB framework that is clearly flexible, as evidenced by the

¹ The fact that this is not immediately consistent with the site occupancies reported by Britton (2003) might be attributed to several factors: (i) the accuracy of the calculations; (ii) the calculations are static and do not consider entropic contributions that must become relevant at real temperatures; (iii) the DMSO orientations may be established during crystal growth, and not solely determined by their relative interaction energies.

existence of the three closely-related framework structures reported herein, and with little consequence for the total energy of the DMSO–TFDIB interactions.

4. Conclusion

The existence of TFDIB–DMSO form II and the variation of the form I structure as a function of temperature shows that the layered arrangement of TFDIB molecules can exhibit significant flexibility in the crystalline state. This flexibility accommodates several orientations for the DMSO molecules between the layers, with apparently little variation in the DMSO–TFDIB interaction energies. The DMSO molecules are consistently anchored by accepting $\text{I} \cdots \text{O}$ halogen bonds, but their orientation can vary relative to the TFDIB molecules and relative to each other. The *PIXEL* calculations suggest no clear preference for orientations **A** or **B** in form I, consistent with the observed disorder in the structure at 297 K, but they show clearly why orientation **C** is preferred in the structure at 120 K. Optimization of the interactions between neighbouring DMSO molecules locks in an ordered arrangement, which accounts for the observed changes in the unit-cell parameters and space group on cooling of form I below *ca* 220 K. The applied combination of temperature-dependent X-ray diffraction measurements and intermolecular energy calculations provides a clear picture of the temperature-dependent phase transformation in this case

Acknowledgements

The cocrystallization study that led to this work was carried out by CLT under the supervision of Professor Stuart Clarke (Department of Chemistry, University of Cambridge).

References

- Accelrys (2011). *Materials Studio*. Accelrys Software Inc., San Diego, CA, USA.
- Blessing, R. H. (1995). *Acta Cryst.* **A51**, 33–38.
- Britton, D. (2003). *Acta Cryst.* **E59**, o1332–o1333.
- Cavallo, G., Metrangolo, P., Milani, R., Pilati, T., Priimagi, A., Resnati, G. & Terraneo, G. (2016). *Chem. Rev.* **116**, 2478–2601.
- Clark, S. J., Segall, M. D., Pickard, C. J., Hasnip, P. J., Probert, M. J., Refson, K. & Payne, M. C. (2005). *Z. Kristallogr.* **220**, 567–570.
- Gavezzotti, A. (2002). *J. Phys. Chem. B*, **106**, 4145–4154.
- Gavezzotti, A. (2003). *J. Phys. Chem. B*, **107**, 2344–2353.
- Gavezzotti, A. (2011). *New J. Chem.* **35**, 1360–1389.
- Grimme, S. (2006). *J. Comput. Chem.* **27**, 1787–1799.
- Groom, C. R., Bruno, I. J., Lightfoot, M. P. & Ward, S. C. (2016). *Acta Cryst.* **B72**, 171–179.
- Macrae, C. F., Sovago, I., Cottrell, S. J., Galek, P. T. A., McCabe, P., Pidcock, E., Platings, M., Shields, G. P., Stevens, J. S., Towler, M. & Wood, P. A. (2020). *J. Appl. Cryst.* **53**, 226–235.
- Metrangolo, P. & Resnati, G. (2001). *Chem. Eur. J.* **7**, 2511–2519.
- Nonius (1998). *COLLECT*. Nonius BV, Delft, The Netherlands.
- Otwinowski, Z. & Minor, W. (1997). *Methods in Enzymology*, Vol. 276, *Macromolecular Crystallography*, Part A, edited by C. W. Carter Jr & R. M. Sweet, pp. 307–326. New York: Academic Press.
- Perdew, J. P., Burke, K. & Ernzerhof, M. (1996). *Phys. Rev. Lett.* **77**, 3865–3868.
- Sheldrick, G. M. (2015a). *Acta Cryst.* **C71**, 3–8.
- Sheldrick, G. M. (2015b). *Acta Cryst.* **A71**, 3–8.

supporting information

Acta Cryst. (2020). C76, 524-529 [https://doi.org/10.1107/S2053229620005690]

Polymorphism and phase transformation in the dimethyl sulfoxide solvate of 2,3,5,6-tetrafluoro-1,4-diiodobenzene

Andrew D. Bond and Chris L. Truscott

Computing details

For all structures, data collection: *COLLECT* (Nonius, 1998); cell refinement: *HKL SCALEPACK* (Otwinowski & Minor, 1997); data reduction: *HKL DENZO* and *SCALEPACK* (Otwinowski & Minor, 1997); program(s) used to solve structure: *SHELXT* (Sheldrick, 2015a); program(s) used to refine structure: *SHELXL2018* (Sheldrick, 2015b); molecular graphics: *Mercury* (Macrae *et al.*, 2020); software used to prepare material for publication: *SHELXL2018* (Sheldrick, 2015b).

2,3,5,6-Tetrafluoro-1,4-diiodobenzene dimethyl sulfoxide (Form_II)

Crystal data

$C_6F_4I_2 \cdot C_2H_6OS$

$M_r = 479.99$

Orthorhombic, *Pnma*

$a = 12.8308$ (6) Å

$b = 21.3307$ (12) Å

$c = 4.6463$ (2) Å

$V = 1271.65$ (11) Å³

$Z = 4$

$F(000) = 880$

$D_x = 2.507$ Mg m⁻³

Mo $K\alpha$ radiation, $\lambda = 0.71073$ Å

Cell parameters from 21867 reflections

$\theta = 1.0$ – 27.5°

$\mu = 5.14$ mm⁻¹

$T = 180$ K

Block, colourless

$0.14 \times 0.14 \times 0.14$ mm

Data collection

Nonius KappaCCD
diffractometer

Radiation source: fine-focus sealed tube

ω and φ -scans

Absorption correction: multi-scan
(SORTAV; Blessing, 1995)

$T_{\min} = 0.411$, $T_{\max} = 0.464$

7999 measured reflections

1463 independent reflections

952 reflections with $I > 2\sigma(I)$

$R_{\text{int}} = 0.049$

$\theta_{\max} = 27.5^\circ$, $\theta_{\min} = 3.7^\circ$

$h = -16 \rightarrow 16$

$k = -27 \rightarrow 21$

$l = -6 \rightarrow 6$

Refinement

Refinement on F^2

Least-squares matrix: full

$R[F^2 > 2\sigma(F^2)] = 0.033$

$wR(F^2) = 0.086$

$S = 1.01$

1463 reflections

83 parameters

0 restraints

Primary atom site location: dual

Secondary atom site location: difference Fourier
map

Hydrogen site location: inferred from
neighbouring sites

H-atom parameters constrained

$w = 1/[\sigma^2(F_o^2) + (0.0432P)^2]$

where $P = (F_o^2 + 2F_c^2)/3$

$(\Delta/\sigma)_{\max} = 0.001$

$\Delta\rho_{\max} = 1.01$ e Å⁻³

$\Delta\rho_{\min} = -1.26$ e Å⁻³

Special details

Geometry. All esds (except the esd in the dihedral angle between two l.s. planes) are estimated using the full covariance matrix. The cell esds are taken into account individually in the estimation of esds in distances, angles and torsion angles; correlations between esds in cell parameters are only used when they are defined by crystal symmetry. An approximate (isotropic) treatment of cell esds is used for estimating esds involving l.s. planes.

Fractional atomic coordinates and isotropic or equivalent isotropic displacement parameters (\AA^2)

	<i>x</i>	<i>y</i>	<i>z</i>	$U_{\text{iso}}^*/U_{\text{eq}}$	Occ. (<1)
I1	0.38600 (2)	0.63930 (2)	0.24280 (5)	0.03540 (15)	
F3	0.69292 (19)	0.46774 (12)	0.1884 (5)	0.0431 (7)	
F2	0.60539 (19)	0.57331 (13)	0.3762 (7)	0.0494 (7)	
C1	0.4543 (3)	0.55611 (18)	0.0978 (9)	0.0299 (10)	
C2	0.5514 (3)	0.5373 (2)	0.1889 (9)	0.0337 (10)	
C3	0.5972 (3)	0.4832 (2)	0.0928 (9)	0.0341 (10)	
S1	0.1684 (3)	0.750000	0.5001 (8)	0.0401 (14)	0.424 (5)
O1	0.2819 (4)	0.750000	0.4285 (11)	0.0624 (15)	0.424 (5)
C4	0.1438 (4)	0.8137 (3)	0.7210 (9)	0.0539 (16)	0.424 (5)
H4A	0.069619	0.814606	0.770785	0.081*	0.424 (5)
H4B	0.185406	0.810022	0.897090	0.081*	0.424 (5)
H4C	0.162495	0.852417	0.620054	0.081*	0.424 (5)
S1A	0.2350 (2)	0.750000	0.7040 (6)	0.0357 (10)	0.576 (5)
O1A	0.2819 (4)	0.750000	0.4285 (11)	0.0624 (15)	0.576 (5)
C4A	0.1438 (4)	0.8137 (3)	0.7210 (9)	0.0539 (16)	0.576 (5)
H4D	0.110604	0.814285	0.910876	0.081*	0.576 (5)
H4E	0.180572	0.853344	0.689187	0.081*	0.576 (5)
H4F	0.090487	0.808153	0.572122	0.081*	0.576 (5)

Atomic displacement parameters (\AA^2)

	U^{11}	U^{22}	U^{33}	U^{12}	U^{13}	U^{23}
I1	0.0367 (2)	0.0246 (2)	0.0449 (3)	0.00355 (11)	0.00368 (13)	-0.00443 (13)
F3	0.0317 (14)	0.0379 (16)	0.0597 (16)	0.0061 (12)	-0.0097 (12)	-0.0088 (12)
F2	0.0490 (15)	0.0381 (17)	0.0610 (18)	0.0041 (13)	-0.0148 (14)	-0.0193 (16)
C1	0.028 (2)	0.022 (2)	0.039 (3)	0.0015 (19)	0.005 (2)	-0.0002 (19)
C2	0.037 (2)	0.027 (2)	0.037 (3)	-0.004 (2)	-0.0025 (19)	-0.003 (2)
C3	0.031 (2)	0.034 (3)	0.038 (3)	0.001 (2)	-0.002 (2)	0.000 (2)
S1	0.053 (3)	0.032 (2)	0.035 (2)	0.000	0.006 (2)	0.000
O1	0.067 (3)	0.026 (3)	0.094 (4)	0.000	0.045 (3)	0.000
C4	0.050 (3)	0.045 (4)	0.066 (4)	0.011 (3)	0.011 (2)	-0.009 (3)
S1A	0.0364 (17)	0.0259 (16)	0.045 (2)	0.000	-0.0053 (13)	0.000
O1A	0.067 (3)	0.026 (3)	0.094 (4)	0.000	0.045 (3)	0.000
C4A	0.050 (3)	0.045 (4)	0.066 (4)	0.011 (3)	0.011 (2)	-0.009 (3)

Geometric parameters (\AA , $^\circ$)

I1—C1	2.090 (4)	S1—C4	1.731 (6)
I1—O1	2.847 (2)	C4—H4A	0.9800

F3—C3	1.347 (5)	C4—H4B	0.9800
F2—C2	1.351 (5)	C4—H4C	0.9800
C1—C2	1.376 (6)	S1A—O1A	1.414 (5)
C1—C3 ⁱ	1.386 (6)	S1A—C4A	1.794 (6)
C2—C3	1.371 (6)	C4A—H4D	0.9800
S1—O1	1.494 (6)	C4A—H4E	0.9800
S1—C4 ⁱⁱ	1.731 (6)	C4A—H4F	0.9800
C1—I1—O1	176.73 (14)	S1—C4—H4A	109.5
C2—C1—C3 ⁱ	116.9 (4)	S1—C4—H4B	109.5
C2—C1—I1	121.8 (3)	H4A—C4—H4B	109.5
C3 ⁱ —C1—I1	121.3 (3)	S1—C4—H4C	109.5
F2—C2—C3	118.0 (4)	H4A—C4—H4C	109.5
F2—C2—C1	119.8 (4)	H4B—C4—H4C	109.5
C3—C2—C1	122.2 (4)	O1A—S1A—C4A	108.5 (2)
F3—C3—C2	119.3 (4)	S1A—C4A—H4D	109.5
F3—C3—C1 ⁱ	119.8 (4)	S1A—C4A—H4E	109.5
C2—C3—C1 ⁱ	120.9 (4)	H4D—C4A—H4E	109.5
O1—S1—C4 ⁱⁱ	108.1 (3)	S1A—C4A—H4F	109.5
O1—S1—C4	108.1 (3)	H4D—C4A—H4F	109.5
C4 ⁱⁱ —S1—C4	103.3 (4)	H4E—C4A—H4F	109.5
S1—O1—I1	121.65 (11)		
C3 ⁱ —C1—C2—F2	-179.5 (4)	C1—C2—C3—F3	179.4 (4)
I1—C1—C2—F2	-0.3 (6)	F2—C2—C3—C1 ⁱ	179.5 (4)
C3 ⁱ —C1—C2—C3	1.4 (7)	C1—C2—C3—C1 ⁱ	-1.5 (8)
I1—C1—C2—C3	-179.4 (3)	C4 ⁱⁱ —S1—O1—I1	47.4 (4)
F2—C2—C3—F3	0.3 (6)	C4—S1—O1—I1	158.6 (3)

Symmetry codes: (i) $-x+1, -y+1, -z$; (ii) $x, -y+3/2, z$.

2,3,5,6-Tetrafluoro-1,4-diiodobenzene dimethyl sulfoxide (Form_I_120K)

Crystal data

$C_6F_4I_2 \cdot C_2H_6OS$
 $M_r = 479.99$
 Orthorhombic, $P2_12_12_1$
 $a = 10.6731$ (2) Å
 $b = 18.0023$ (5) Å
 $c = 6.5470$ (2) Å
 $V = 1257.94$ (5) Å³
 $Z = 4$
 $F(000) = 880$

$D_x = 2.534$ Mg m⁻³
 Mo $K\alpha$ radiation, $\lambda = 0.71073$ Å
 Cell parameters from 22578 reflections
 $\theta = 1.0$ – 27.5°
 $\mu = 5.19$ mm⁻¹
 $T = 120$ K
 Block, colourless
 $0.12 \times 0.10 \times 0.10$ mm

Data collection

Nonius KappaCCD
 diffractometer
 Radiation source: fine-focus sealed tube
 ω and ϕ -scans
 Absorption correction: multi-scan
 (SORTAV; Blessing, 1995)

$T_{\min} = 0.475$, $T_{\max} = 0.599$
 11512 measured reflections
 2834 independent reflections
 2141 reflections with $I > 2\sigma(I)$
 $R_{\text{int}} = 0.089$
 $\theta_{\max} = 27.5^\circ$, $\theta_{\min} = 3.7^\circ$

$h = -13 \rightarrow 13$
 $k = -22 \rightarrow 22$

$l = -8 \rightarrow 8$

Refinement

Refinement on F^2
 Least-squares matrix: full
 $R[F^2 > 2\sigma(F^2)] = 0.043$
 $wR(F^2) = 0.078$
 $S = 0.99$
 2834 reflections
 148 parameters
 0 restraints
 Primary atom site location: dual
 Secondary atom site location: difference Fourier map

Hydrogen site location: inferred from neighbouring sites
 H-atom parameters constrained
 $w = 1/[\sigma^2(F_o^2) + (0.0294P)^2]$
 where $P = (F_o^2 + 2F_c^2)/3$
 $(\Delta/\sigma)_{\max} < 0.001$
 $\Delta\rho_{\max} = 0.91 \text{ e } \text{\AA}^{-3}$
 $\Delta\rho_{\min} = -1.17 \text{ e } \text{\AA}^{-3}$
 Absolute structure: Refined as an inversion twin.
 Absolute structure parameter: 0.19 (5)

Special details

Geometry. All esds (except the esd in the dihedral angle between two l.s. planes) are estimated using the full covariance matrix. The cell esds are taken into account individually in the estimation of esds in distances, angles and torsion angles; correlations between esds in cell parameters are only used when they are defined by crystal symmetry. An approximate (isotropic) treatment of cell esds is used for estimating esds involving l.s. planes.

Refinement. Refined as a 2-component inversion twin.

Fractional atomic coordinates and isotropic or equivalent isotropic displacement parameters (\AA^2)

	<i>x</i>	<i>y</i>	<i>z</i>	$U_{\text{iso}}^*/U_{\text{eq}}$
I1	0.16341 (6)	0.65366 (4)	-0.30645 (10)	0.0241 (2)
I4	-0.11363 (6)	0.38880 (4)	0.33529 (10)	0.0238 (2)
F2	-0.0772 (5)	0.5501 (3)	-0.3553 (8)	0.0258 (15)
F3	-0.1813 (6)	0.4475 (4)	-0.1158 (8)	0.0286 (16)
F5	0.1268 (5)	0.4943 (3)	0.3876 (9)	0.0263 (16)
F6	0.2318 (5)	0.5959 (3)	0.1467 (8)	0.0265 (15)
C1	0.0822 (10)	0.5744 (6)	-0.1121 (15)	0.023 (3)
C2	-0.0242 (9)	0.5361 (6)	-0.1730 (16)	0.020 (2)
C3	-0.0796 (10)	0.4838 (7)	-0.0479 (17)	0.025 (3)
C4	-0.0315 (10)	0.4683 (6)	0.1451 (16)	0.022 (3)
C5	0.0748 (10)	0.5076 (6)	0.2036 (16)	0.021 (2)
C6	0.1290 (10)	0.5591 (6)	0.0776 (15)	0.024 (3)
S1	0.3629 (3)	0.79817 (17)	0.3362 (4)	0.0283 (7)
O1	0.2421 (7)	0.7752 (4)	0.4393 (10)	0.027 (2)
C7	0.4693 (12)	0.7225 (8)	0.3733 (18)	0.046 (4)
H7A	0.496485	0.721303	0.516269	0.068*
H7B	0.542462	0.728983	0.284566	0.068*
H7C	0.427306	0.675658	0.339413	0.068*
C8	0.3380 (12)	0.7839 (7)	0.0711 (16)	0.036 (3)
H8A	0.305056	0.733741	0.048777	0.054*
H8B	0.417497	0.789565	-0.002088	0.054*
H8C	0.277613	0.820520	0.020317	0.054*

Atomic displacement parameters (\AA^2)

	U^{11}	U^{22}	U^{33}	U^{12}	U^{13}	U^{23}
I1	0.0231 (4)	0.0235 (4)	0.0257 (4)	-0.0015 (3)	0.0009 (3)	0.0009 (3)
I4	0.0259 (4)	0.0216 (4)	0.0239 (3)	-0.0010 (3)	0.0026 (3)	0.0003 (3)
F2	0.026 (3)	0.028 (4)	0.024 (3)	0.001 (3)	-0.006 (3)	0.001 (3)
F3	0.025 (4)	0.033 (4)	0.028 (3)	-0.004 (3)	-0.003 (3)	-0.002 (3)
F5	0.024 (4)	0.028 (4)	0.027 (3)	0.001 (3)	-0.001 (3)	0.001 (3)
F6	0.024 (3)	0.027 (4)	0.028 (3)	-0.006 (3)	-0.002 (3)	-0.003 (3)
C1	0.025 (7)	0.016 (6)	0.027 (6)	-0.003 (5)	0.006 (5)	-0.009 (5)
C2	0.014 (5)	0.030 (7)	0.017 (5)	0.008 (5)	0.002 (5)	-0.007 (6)
C3	0.020 (6)	0.030 (8)	0.025 (6)	-0.003 (6)	0.004 (5)	0.001 (5)
C4	0.024 (6)	0.020 (7)	0.021 (6)	0.009 (5)	0.002 (5)	-0.004 (5)
C5	0.020 (6)	0.020 (6)	0.023 (6)	0.003 (5)	0.000 (5)	0.004 (5)
C6	0.022 (7)	0.024 (7)	0.026 (5)	0.004 (6)	-0.009 (5)	-0.016 (5)
S1	0.0264 (17)	0.0278 (17)	0.0306 (14)	-0.0038 (13)	0.0005 (14)	-0.0076 (14)
O1	0.027 (5)	0.028 (5)	0.026 (4)	0.005 (4)	0.009 (4)	0.003 (4)
C7	0.042 (9)	0.058 (11)	0.037 (8)	0.020 (7)	-0.006 (7)	0.005 (7)
C8	0.033 (7)	0.051 (10)	0.024 (6)	-0.002 (7)	0.002 (6)	0.005 (6)

Geometric parameters (\AA , $^\circ$)

I1—C1	2.099 (11)	C4—C5	1.391 (15)
I1—O1 ⁱ	2.874 (7)	C5—C6	1.369 (15)
I4—C4	2.090 (11)	S1—O1	1.513 (8)
I4—O1 ⁱⁱ	2.871 (7)	S1—C8	1.774 (11)
F2—C2	1.344 (11)	S1—C7	1.791 (13)
F3—C3	1.343 (12)	C7—H7A	0.9800
F5—C5	1.348 (12)	C7—H7B	0.9800
F6—C6	1.359 (12)	C7—H7C	0.9800
C1—C6	1.367 (14)	C8—H8A	0.9800
C1—C2	1.387 (15)	C8—H8B	0.9800
C2—C3	1.381 (15)	C8—H8C	0.9800
C3—C4	1.392 (15)		
C1—I1—O1 ⁱ	171.5 (3)	F6—C6—C5	118.1 (9)
C4—I4—O1 ⁱⁱ	174.0 (3)	C1—C6—C5	122.0 (10)
C6—C1—C2	117.4 (11)	O1—S1—C8	105.6 (5)
C6—C1—I1	122.5 (9)	O1—S1—C7	105.8 (6)
C2—C1—I1	120.1 (8)	C8—S1—C7	96.8 (6)
F2—C2—C3	118.3 (9)	S1—C7—H7A	109.5
F2—C2—C1	120.4 (10)	S1—C7—H7B	109.5
C3—C2—C1	121.3 (10)	H7A—C7—H7B	109.5
F3—C3—C2	118.8 (10)	S1—C7—H7C	109.5
F3—C3—C4	120.1 (10)	H7A—C7—H7C	109.5
C2—C3—C4	121.1 (11)	H7B—C7—H7C	109.5
C5—C4—C3	116.7 (10)	S1—C8—H8A	109.5
C5—C4—I4	121.8 (8)	S1—C8—H8B	109.5

C3—C4—I4	121.5 (8)	H8A—C8—H8B	109.5
F5—C5—C6	119.1 (9)	S1—C8—H8C	109.5
F5—C5—C4	119.4 (9)	H8A—C8—H8C	109.5
C6—C5—C4	121.5 (10)	H8B—C8—H8C	109.5
F6—C6—C1	119.9 (10)		
C6—C1—C2—F2	178.1 (9)	C3—C4—C5—F5	-179.0 (9)
I1—C1—C2—F2	-0.9 (13)	I4—C4—C5—F5	0.0 (13)
C6—C1—C2—C3	-0.9 (16)	C3—C4—C5—C6	0.3 (16)
I1—C1—C2—C3	-179.9 (9)	I4—C4—C5—C6	179.3 (8)
F2—C2—C3—F3	2.1 (16)	C2—C1—C6—F6	-178.9 (9)
C1—C2—C3—F3	-178.9 (9)	I1—C1—C6—F6	0.1 (14)
F2—C2—C3—C4	-178.1 (9)	C2—C1—C6—C5	0.7 (16)
C1—C2—C3—C4	0.9 (17)	I1—C1—C6—C5	179.6 (8)
F3—C3—C4—C5	179.3 (9)	F5—C5—C6—F6	-1.5 (15)
C2—C3—C4—C5	-0.6 (16)	C4—C5—C6—F6	179.2 (9)
F3—C3—C4—I4	0.2 (15)	F5—C5—C6—C1	178.9 (9)
C2—C3—C4—I4	-179.6 (8)	C4—C5—C6—C1	-0.3 (17)

Symmetry codes: (i) $x, y, z-1$; (ii) $-x, y-1/2, -z+1$.

2,3,5,6-Tetrafluoro-1,4-diiodobenzene dimethyl sulfoxide (Form_I_220K)

Crystal data

$C_6F_4I_2 \cdot C_2H_6OS$

$M_r = 479.99$

Orthorhombic, *Pnma*

$a = 11.6799$ (4) Å

$b = 18.2664$ (8) Å

$c = 6.0984$ (2) Å

$V = 1301.09$ (8) Å³

$Z = 4$

$F(000) = 880$

$D_x = 2.450$ Mg m⁻³

Mo $K\alpha$ radiation, $\lambda = 0.71073$ Å

Cell parameters from 4026 reflections

$\theta = 1.0$ – 27.5°

$\mu = 5.02$ mm⁻¹

$T = 220$ K

Block, colourless

$0.12 \times 0.10 \times 0.10$ mm

Data collection

Nonius KappaCCD
diffractometer

Radiation source: fine-focus sealed tube

ω and φ -scans

Absorption correction: multi-scan
(SORTAV; Blessing, 1995)

$T_{\min} = 0.541$, $T_{\max} = 0.611$

8062 measured reflections

1520 independent reflections

948 reflections with $I > 2\sigma(I)$

$R_{\text{int}} = 0.057$

$\theta_{\max} = 27.5^\circ$, $\theta_{\min} = 3.5^\circ$

$h = -15 \rightarrow 15$

$k = -23 \rightarrow 23$

$l = -7 \rightarrow 7$

Refinement

Refinement on F^2

Least-squares matrix: full

$R[F^2 > 2\sigma(F^2)] = 0.038$

$wR(F^2) = 0.082$

$S = 1.06$

1520 reflections

112 parameters

71 restraints

Primary atom site location: dual

Secondary atom site location: difference Fourier
map

Hydrogen site location: mixed

H-atom parameters constrained

$w = 1/[\sigma^2(F_o^2) + (0.0284P)^2 + 1.1523P]$

where $P = (F_o^2 + 2F_c^2)/3$

$(\Delta/\sigma)_{\max} = 0.001$

$\Delta\rho_{\max} = 0.62$ e Å⁻³

$\Delta\rho_{\min} = -0.68$ e Å⁻³

Extinction correction: (SHELXL2018;
Sheldrick, 2015b)

Extinction coefficient: 0.0132 (6)

Special details

Geometry. All esds (except the esd in the dihedral angle between two l.s. planes) are estimated using the full covariance matrix. The cell esds are taken into account individually in the estimation of esds in distances, angles and torsion angles; correlations between esds in cell parameters are only used when they are defined by crystal symmetry. An approximate (isotropic) treatment of cell esds is used for estimating esds involving l.s. planes.

Fractional atomic coordinates and isotropic or equivalent isotropic displacement parameters (\AA^2)

	x	y	z	$U_{\text{iso}}^*/U_{\text{eq}}$	Occ. (<1)
I1	0.64113 (3)	0.63330 (2)	-0.19139 (6)	0.0723 (2)	
F2	0.4101 (3)	0.54499 (18)	-0.1142 (4)	0.0772 (9)	
F3	0.2989 (3)	0.44527 (19)	-0.3508 (5)	0.0790 (9)	
C1	0.5582 (4)	0.5530 (3)	-0.3749 (8)	0.0581 (13)	
C2	0.4550 (4)	0.5233 (3)	-0.3061 (7)	0.0584 (13)	
C3	0.3987 (4)	0.4720 (3)	-0.4276 (8)	0.0595 (13)	
S1	0.3111 (5)	0.750000	0.2275 (10)	0.0568 (15)	0.356 (3)
O1	0.2370 (5)	0.750000	0.4298 (11)	0.110 (2)	0.356 (3)
C4	0.4068 (8)	0.67661 (19)	0.2756 (19)	0.090 (4)	0.356 (3)
H4A	0.480039	0.687320	0.207791	0.136*	0.356 (3)
H4B	0.375583	0.632042	0.213079	0.136*	0.356 (3)
H4C	0.417218	0.670231	0.432221	0.136*	0.356 (3)
S1A	0.3676 (8)	0.750000	0.4425 (19)	0.067 (3)	0.191 (3)
O1A	0.2370 (5)	0.750000	0.4298 (11)	0.110 (2)	0.191 (3)
C4A	0.4068 (8)	0.67661 (19)	0.2756 (19)	0.090 (4)	0.191 (3)
H4D	0.370704	0.681797	0.133178	0.136*	0.191 (3)
H4E	0.382158	0.631141	0.342851	0.136*	0.191 (3)
H4F	0.489331	0.676074	0.257885	0.136*	0.191 (3)
S1B	0.3538 (6)	0.7203 (5)	0.3374 (15)	0.084 (2)	0.2261 (16)
O1B	0.2370 (5)	0.750000	0.4298 (11)	0.110 (2)	0.452 (3)
C4B	0.334 (2)	0.750000	0.060 (2)	0.137 (10)	0.452 (3)
H4G	0.274509	0.721310	-0.005420	0.205*	0.2261 (16)
H4H	0.312749	0.800730	0.058820	0.205*	0.2261 (16)
H4I	0.403849	0.743630	-0.021090	0.205*	0.2261 (16)
C5B	0.463 (3)	0.7845 (16)	0.405 (5)	0.157 (17)	0.2261 (16)
H5A	0.488010	0.777330	0.553795	0.236*	0.2261 (16)
H5B	0.526850	0.776550	0.307735	0.236*	0.2261 (16)
H5C	0.435739	0.833651	0.387645	0.236*	0.2261 (16)

Atomic displacement parameters (\AA^2)

	U^{11}	U^{22}	U^{33}	U^{12}	U^{13}	U^{23}
I1	0.0789 (3)	0.0640 (3)	0.0739 (3)	-0.00229 (18)	-0.01656 (19)	-0.00687 (17)
F2	0.0743 (19)	0.100 (3)	0.0575 (16)	0.0044 (18)	0.0064 (15)	-0.0184 (16)
F3	0.0617 (18)	0.106 (3)	0.0691 (17)	-0.0177 (18)	0.0025 (16)	0.0027 (17)
C1	0.065 (3)	0.055 (3)	0.055 (3)	0.008 (3)	-0.011 (2)	-0.003 (2)

C2	0.061 (3)	0.063 (3)	0.051 (3)	0.008 (3)	-0.003 (3)	0.002 (2)
C3	0.056 (3)	0.067 (3)	0.055 (3)	-0.003 (3)	-0.003 (3)	0.006 (3)
S1	0.057 (3)	0.070 (4)	0.044 (3)	0.000	0.002 (3)	0.000
O1	0.108 (4)	0.088 (4)	0.133 (5)	0.000	0.056 (4)	0.000
C4	0.068 (6)	0.080 (8)	0.123 (8)	0.015 (6)	0.015 (6)	-0.018 (7)
S1A	0.086 (7)	0.058 (7)	0.055 (6)	0.000	-0.025 (5)	0.000
O1A	0.108 (4)	0.088 (4)	0.133 (5)	0.000	0.056 (4)	0.000
C4A	0.068 (6)	0.080 (8)	0.123 (8)	0.015 (6)	0.015 (6)	-0.018 (7)
S1B	0.086 (5)	0.076 (5)	0.091 (6)	-0.013 (4)	0.021 (4)	0.009 (4)
O1B	0.108 (4)	0.088 (4)	0.133 (5)	0.000	0.056 (4)	0.000
C4B	0.139 (12)	0.140 (13)	0.132 (12)	0.000	-0.003 (9)	0.000
C5B	0.157 (19)	0.16 (2)	0.153 (19)	-0.006 (10)	-0.009 (10)	-0.001 (10)

Geometric parameters (Å, °)

I1—C1	2.083 (5)	C4A—H4E	0.9700
I1—O1 ⁱ	2.888 (4)	C4A—H4F	0.9700
F2—C2	1.342 (5)	S1B—S1B ⁱⁱⁱ	1.085 (18)
F3—C3	1.348 (6)	S1B—C5B ⁱⁱⁱ	1.35 (2)
C1—C3 ⁱⁱ	1.384 (7)	S1B—O1B	1.573 (8)
C1—C2	1.387 (7)	S1B—C5B	1.785 (10)
C2—C3	1.363 (7)	S1B—C4B	1.789 (10)
S1—O1	1.508 (7)	S1B—H4H ⁱⁱⁱ	1.806 (11)
S1—C4 ⁱⁱⁱ	1.770 (7)	C4B—H4G	0.9600
S1—C4	1.770 (7)	C4B—H4H	0.9600
S1—H4G ⁱⁱⁱ	1.573 (12)	C4B—H4I	0.9600
S1—H4H ⁱⁱⁱ	1.385 (10)	C4B—H4G ⁱⁱⁱ	0.9600
C4—H4A	0.9700	C4B—H4H ⁱⁱⁱ	0.9600
C4—H4B	0.9700	C4B—H4I ⁱⁱⁱ	0.9600
C4—H4C	0.9700	C5B—C5B ⁱⁱⁱ	1.26 (6)
S1A—O1A	1.528 (9)	C5B—H5A	0.9600
S1A—C4A	1.744 (8)	C5B—H5B	0.9601
S1A—C4A ⁱⁱⁱ	1.744 (8)	C5B—H5C	0.9600
C4A—H4D	0.9700		
C1—I1—O1 ⁱ	175.05 (18)	S1—C4—H4A	109.5
C3 ⁱⁱ —C1—C2	116.7 (5)	S1—C4—H4B	109.5
C3 ⁱⁱ —C1—I1	122.1 (4)	H4A—C4—H4B	109.5
C2—C1—I1	121.2 (4)	S1—C4—H4C	109.5
F2—C2—C3	119.3 (5)	H4A—C4—H4C	109.5
F2—C2—C1	119.1 (5)	H4B—C4—H4C	109.5
C3—C2—C1	121.6 (5)	O1A—S1A—C4A	103.4 (5)
F3—C3—C2	118.5 (4)	S1A—C4A—H4D	109.5
F3—C3—C1 ⁱⁱ	119.8 (5)	S1A—C4A—H4E	109.5
C2—C3—C1 ⁱⁱ	121.7 (5)	H4D—C4A—H4E	109.5
O1—S1—C4 ⁱⁱⁱ	103.1 (5)	S1A—C4A—H4F	109.5
O1—S1—C4	103.1 (5)	H4D—C4A—H4F	109.5
C4 ⁱⁱⁱ —S1—C4	98.5 (6)	H4E—C4A—H4F	109.5

C3 ⁱⁱ —C1—C2—F2	179.1 (4)	F2—C2—C3—F3	0.5 (7)
I1—C1—C2—F2	-2.3 (6)	C1—C2—C3—F3	179.8 (4)
C3 ⁱⁱ —C1—C2—C3	-0.2 (8)	F2—C2—C3—C1 ⁱⁱ	-179.1 (4)
I1—C1—C2—C3	178.4 (4)	C1—C2—C3—C1 ⁱⁱ	0.2 (8)

Symmetry codes: (i) $x+1/2, y, -z+1/2$; (ii) $-x+1, -y+1, -z-1$; (iii) $x, -y+3/2, z$.